ACS Macro Letters

pubs.acs.org/macroletters Letter

Large-Scale Centrifugal Multispinning Production of Polymer Micro- and Nanofibers for Mask Filter Application with a Potential of Cospinning Mixed Multicomponent Fibers

Byeong Eun Kwak, Hyo Jeong Yoo, Eungjun Lee, and Do Hyun Kim*

Cite This: ACS Macro Lett. 2021, 10, 382−388 Read Online

ACCESS | Metrics & More | Article Recommendations | Supporting Information

ABSTRACT: Recently, the polymer nanofiber web is in high demand as a strong barrier against harmful particles due to its high capture efficiency and strong droplet-blocking ability. As an advanced spinning technique, the centrifugal multispinning system was designed by sectioning a rotating disk into triple subdisks, showing mass producibility of polymer nanofibers with cospinning ability. Using the system, gram-scale production of polystyrene (PS), poly(methyl methacrylate), and polyvinylpyrrolidone (PVP) was demonstrated, showing a possibility for versatile use of the system. Moreover, a high production rate of ∼25 g/h for PS nanofibers was achieved, which is ∼300× higher than that of the usual electrospinning process. Utilizing the cospinning ability, we controlled the contact angle and electrostatic charge of the multicomponent nanofiber web by adjusting the relative amounts of PS and PVP fibers, showing a potential for functional textile application. With the fabricated PS nanofiber-based filters, we achieved high capture efficiency up to ∼97% with outstanding droplet-blocking ability.

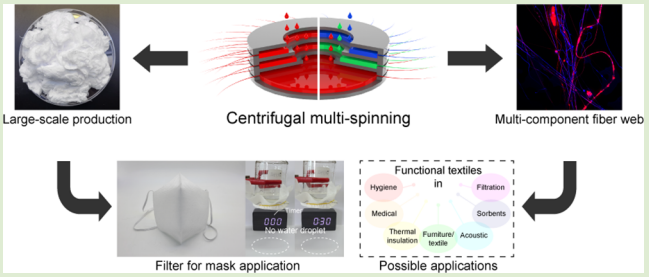

The importance of a mask filter has been highlighted because of fine dust and coronavirus disease-2019 (COVID-19), which are urgent issues in human health.[1−3] A polymer nanofiber-based filter can act as an effective barrier against dust and virus-containing droplets since it can show high capture efficiency and excellent blocking ability against water droplets arising from their fine network and hydrophobicity.[4−6] Electrospinning is a routine way to prepare nanofiber webs, but in terms of mass production, it has several drawbacks, such as low throughput, the requirement of an electrically conductive target, a safety problem resulting from high voltage, and the difficulty of scale-up.[7−9]

Centrifugal spinning is a strong candidate for the mass production of polymer micro- and nanofibers because of its advantages, including high production rate, cost effectiveness, and no need for high voltage and an electrically conductive target.[10,11] With this useful feature, centrifugal spinning has the potential to be employed not only for mass production of polymer micro- and nanofibers, but also for versatile processes such as aligned fiber spinning,[12−18] but still with room for improvement. The recent trend in centrifugal spinning research is mainly focused on the integration between centrifugal spinning and electrospinning processes, using centrifugal force as the supporting force rather than the main driving force to prepare fibers.[12,19−21] This limited research trend restricts further enhancement of the productivity of centrifugal spinning since a high-voltage electrical system in this research limits the scalability of the system. The spinneret is a key component that determines the morphology and production rate of fibers in a centrifugal spinning system. The use of multiple spinnerets can directly lead to the scalability of the spinning system, but most research employed a single spinneret.[22−25] Employment of multiple spinnerets can also allow us to form multicomponent nanofiber webs with fine control of their physical and chemical properties for various applications such as drug delivery,[12] tissue engineering,[26] and functional textile applications.[27,28]

Inspired by those strengths, we designed a centrifugal multispinning system for the large-scale production of polymer micro- and nanofibers with a potential of cospinning mixed multicomponent fibers. As a strategy to multiplicate the spinneret, we sectioned a rotating disk into three subdisks that are vertically integrated together, and the subdisks were rotated simultaneously with a single axis.

With the novel spinneret, we set the spinning system as shown in Figure 1A. The inset displays the detailed structure of the multispinning disk consisting of three subdisks. Polymer solutions were ejected through the gaps at the side wall of each subdisk. Before the multispinning, which is more complicated

Received: November 29, 2020
Accepted: February 10, 2021
Published: February 17, 2021

https://dx.doi.org/10.1021/acsmacrolett.0c00829
ACS Macro Lett. 2021, 10, 382−388

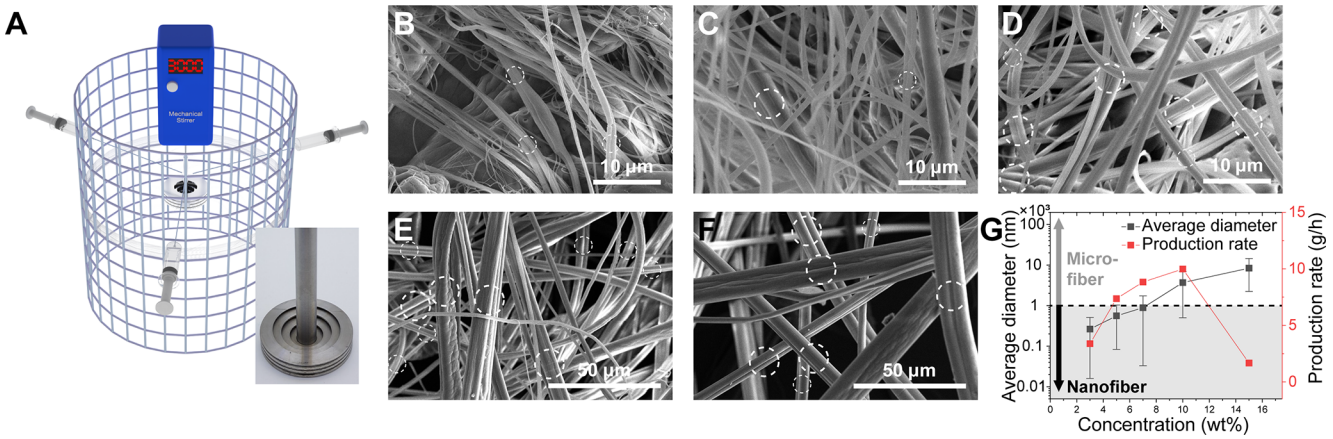

Figure 1. Centrifugal spinning of PS fibers using a single subdisk. (A) Experimental setup and the centrifugal multispinning disk (right). SEM images of the prepared PS fibers at the concentrations of (B) 3 wt %, (C) 5 wt %, (D) 7 wt %, (E) 10 wt %, and (F) 15 wt %. (G) Average diameter and production rate of PS fibers with different concentrations.

than normal centrifugal spinning, we first optimized the polymer concentration using a single subdisk for simplicity. We prepared polystyrene (PS) polymer solutions by dissolving PS in chloroform with different concentrations of 3, 5, 7, 10, and 15 wt %, followed by centrifugal spinning. Scanning electron microscopy (SEM) images show that PS fibers were successfully prepared (Figure 1B–F). Since the fiber diameter is the most important factor for the mass production of nanofibers, we focused on it as a necessary criterion to optimize the concentration. Additionally, the production rate is another consideration, so the two values at each concentration are summarized in Figure 1G.

Average diameters of the PS fibers were measured as 263 ± 247, 558 ± 475, 888 ± 855, 3688 ± 3186, and 8372 ± 6134 nm at the concentrations of 3, 5, 7, 10, and 15 wt %, respectively. Fiber diameter distributions were shown in Figure S1. At concentrations higher than 5 wt %, the prepared fibers have extremely large diameters compared to other electrospinning processes (100–650 nm; Table S1),[29−50] while the average diameter at concentrations of 3 and 5 wt % is similar to that of electrospun fibers. The results clearly show that a higher concentration induced the formation of fibers with larger diameters. This increase in diameter along the concentration is due to the high viscosity and reduced contents of solvent, which are evaporated during the spinning, further limiting the elongation of the polymer jets.[51,52] Moreover, merged fibers indicated as dashed circles in SEM images are more frequently observed in higher concentrations larger than 5 wt %, which leads to dramatic increase of average fiber diameter. Thus, a lower concentration is more appropriate for preparing nanofibers. Meanwhile, the production rate of the PS fibers was calculated as 3.38, 7.368, 8.832, 9.984, and 1.67 g/h at the concentrations of 3, 5, 7, 10, and 15 wt %, respectively, showing an increase along the concentration and a sudden decrease at the concentration of 15 wt %, which is a different trend with the fiber diameter. In higher concentrations, since the resultant polymer jets have a smaller surface area, the solvent evaporation was further retarded, forming concentrated droplets and imperfectly solidified fibers rather than a fibrous network. Those solvent-containing structures can destroy the preformed fibers at the collector by fusion, so more formation of those structures may limit the further enhancement of the production rate at higher concentrations. Considering both factors, we selected 5 wt % PS solution as a base solution since it can dominantly provide nanofibers rather than microfibers with a high production rate.

To demonstrate the applicability of our system for the fiber preparation with various polymers, poly(methyl methacrylate) (PMMA) and polyvinylpyrrolidone (PVP), which are frequently employed in various applications,[53−58] were also spun in the same way. PMMA and PVP were dissolved in chloroform and ethanol, respectively, with various concentrations. SEM images show that PMMA and PVP fibers were successfully prepared (Figures S2 and S3). The prepared PMMA fibers showed a similar trend with PS, producing fibers with a larger diameter at a higher concentration, while the results of PVP spinning demonstrate a narrower concentration window. PMMA and PVP have the highest production rates of 6.516 and 1.77 g/h at 5 and 7 wt % concentrations, respectively, showing a potential of centrifugal spinning for gram-scale production of polymer nanofibers. These results also demonstrate that the centrifugal spinning system can produce various polymer micro- and nanofibers, regardless of their chemical and physical properties.

Before expansion from normal centrifugal spinning to centrifugal multispinning, the performance of each subdisk should be cross-checked in terms of average diameter and morphology of fibers since all the aforementioned results are obtained using the single subdisk. Therefore, we prepared PS nanofibers by each subdisk and examined whether all the subdisks can produce the same results or not (Figure S4). Consequently, there is no morphology change of the resultant nanofibers, and only small deviation of average fiber diameter was observed for each subdisk, showing negligible influence of different injection locations. It may be due to that polymer solutions in subdisk are accelerated for extremely short time with negligible difference until ejection. Thus, we could expect the same performance of centrifugal multispinning with that of single spinning, just increasing the production rate of the nanofibers.

To assess the effectiveness of the centrifugal multispinning system for mass production of the nanofiber, we adopted an electrospinning process as a conventional spinning method and compared its production rate with that of our system. We used the PS solution with the same concentration range from 3 to 15 wt %, and we varied the feed flow rate from 0.5 to 8 mL/h

https://dx.doi.org/10.1021/acsmacrolett.0c00829
ACS Macro Lett. 2021, 10, 382−388

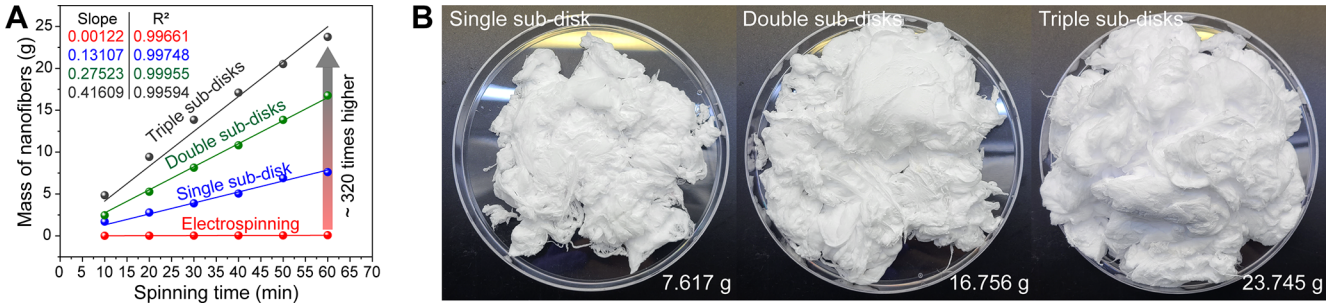

Figure 2. Production rate calculation of PS nanofibers. (A) Weight of nanofibers that were spun by centrifugal spinning and electrospinning according to spinning time. (B) Photographs of the prepared PS nanofibers spun by centrifugal multispinning with a different number of subdisks.

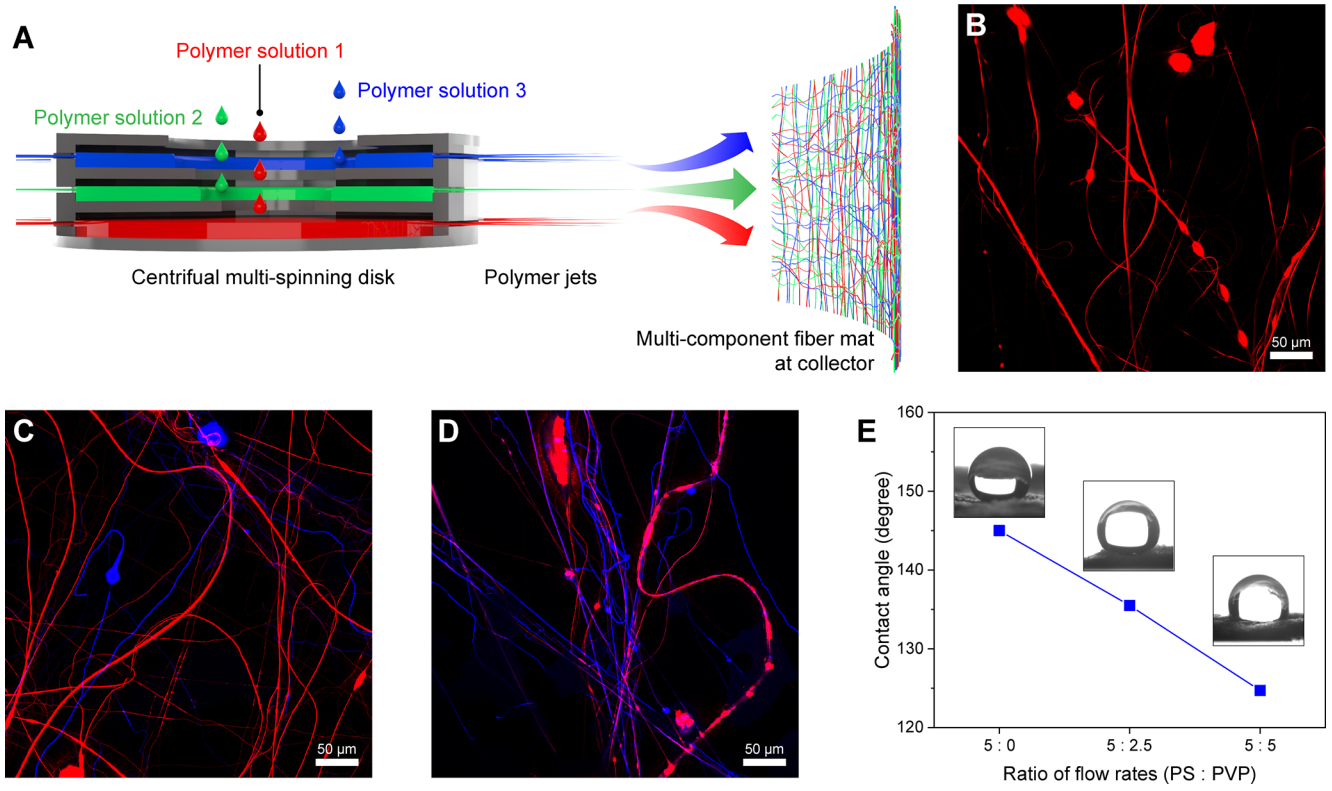

Figure 3. Centrifugal multispinning of different polymers. (A) Schematic illustration of centrifugal multispinning using three different polymer solutions. Confocal laser scanning microscope images of the cospun PS and PVP nanofibers with flow rate ratios (PS/PVP) of (B) 5:0, (C) 5:2.5, and (D) 5:5. The PS solution was mixed with rhodamine B (red in the image), and the PVP solution was mixed with carbon dots (blue in the image). (E) Contact angle of spun nanofiber webs with different ratios of flow rates of PS and PVP solutions. Deionized water was used to measure the contact angle.

to find the maximum production rate at each concentration (Figures S5−S9). Based on the results, we selected the adequate condition for the production of electrospun fibers by removing cases that produce only beads without fibers or a molten area. The fiber diameter and the production rate for each case are summarized in Figure S10. Since we selected the 5 wt % PS solution as a base solution for centrifugal spinning, we compared the nanofiber production rate between the two systems employing this concentration (Figure 2A). At 5 wt % concentration, the maximum production rate was measured as 0.078 g/h for a single-syringe electrospinning system, while the centrifugal spinning system produced 7.864 g of nanofibers per hour. Moreover, with an increase in the number of subdisks, the production rate was further enhanced by 16.514 and 24.965 g/h for double- and triple-subdisk cases, respectively (Figure 2B). As a result, a centrifugal multispinning system showed an extremely enhanced production rate of over ∼300× compared to the electrospinning system with the same solution condition. Although the case of 7 wt % concentration with a feed flow rate of 5 mL/h recorded the maximum production rate of 0.606 g/h for the electrospinning system, the nanofiber production rate of the centrifugal multispinning system is still 41× higher than that value. We also compared the production rate with that of other multinozzle or needleless electrospinning processes (Table S1). While most mass-producible electrospinning systems showed low productivity of a few grams per hour, some processes showed a high productivity of ∼20−40 g/h,[36,40] which is comparable to that of the centrifugal multispinning process. However, in the comparison of productivity per unit spinneret, our centrifugal multispinning system still has a relatively high productivity of ∼8.3 g/h·subdisk, compared to that of the processes (∼0.20−4.6 g/

https://dx.doi.org/10.1021/acsmacrolett.0c00829
ACS Macro Lett. 2021, 10, 382−388

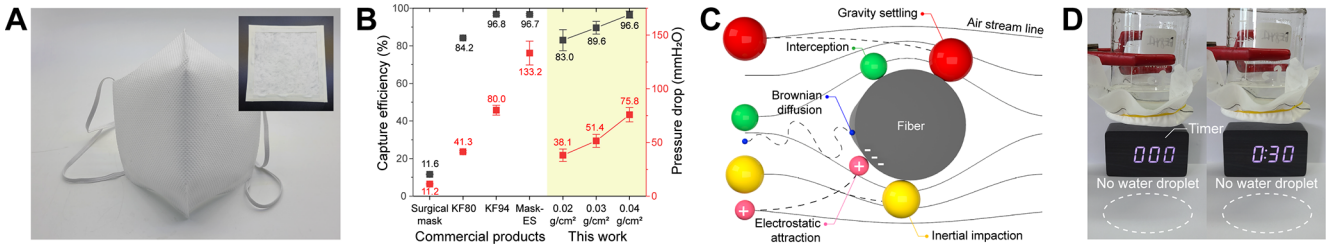

Figure 4. Mask filter application of PS nanofibers. (A) The fabricated PS nanofiber-based mask for fine dust capture and filter for measurements of capture efficiency and resistance (inset). (B) Capture efficiency and resistance of the fabricated filters according to the weight of the nanofiber per unit area compared to commercial products. (C) Filtration mechanisms of air filter. (D) Test for water droplet-blocking ability of the PS nanofiber-based mask filter. The test was performed for 30 min.

h·spinneret). This overwhelmingly higher value in the production rate than that of the electrospinning system clearly demonstrates a potential of our system for producing nanofibers. Moreover, analogous to multinozzle electrospinning system, the productivity of the centrifugal multispinning system can be further enhanced by an integration of more subdisks, showing easy scalability of our system.

Besides mass production, we employed centrifugal multispinning for cospinning different polymer species to expand the application of polymer nanofibers. Figure 3A shows a schematic illustration for the preparation of a multicomponent nanofiber web. Three types of polymer solutions were injected to each subdisk, and each polymer solution can be ejected by centrifugal force. After elongation and solvent evaporation, polymer jets become nanofibers, and consequently, a multicomponent nanofiber web can be fabricated. Since the multicomponent fiber web consists of different types of polymers, its physical and chemical properties can be finely tuned by controlling the relative amounts of different polymer fibers. To demonstrate the practical preparation of multicomponent nanofiber webs, we selected two polymer solutions, 5 wt % PS in chloroform and 7 wt % PVP in ethanol, which are hydrophobic and hydrophilic, respectively. The 7 wt % concentration of PVP solution was chosen to prepare nanofibers having similar diameters with that of the PS nanofibers. For fine control of physical and chemical properties of bicomponent nanofiber web, relative amounts of two polymers should be controlled. To produce different amounts of nanofibers without changing fiber quality, we controlled the feed flow rate of PVP solution. Since the injected solution drops experienced the same centrifugal force, it does not affect the average diameter and morphology of the prepared nanofibers (Figure S11). Thus, we varied the feed flow rate of the PVP solution from 0 to 5 mL/min to control the ratio of PS and PVP nanofibers within multicomponent fiber webs. To visualize each type of nanofiber, rhodamine B and blue-emitting carbon dots were mixed with PS and PVP solutions, respectively, and each solution was injected to different subdisks.

Without an injection of the PVP solution, only PS fibers (red color) were spun as shown in Figure 3B. As the flow rate of the PVP solution increased, the amount of PVP fibers (blue color) increased (Figure 3C,D). The confocal images demonstrate that two polymer solutions were not mixed during the spinning process forming the bicomponent nanofiber webs. When two polymer solutions were injected into the same subdisk, most fibers showed a purple-color emission (Figure S12), implying that the mixing of two solutions occurred during the spinning. It shows that each chamber for the spinning solutions should be sectioned to prevent mixing of different solutions for the preparation of multicomponent fiber webs. Among many characteristics of the webs, the contact angle and electrostatic charge were measured (Figures 3E and S13). Due to the hydrophilicity of the PVP nanofibers, the contact angle gradually decreased as the amount of PVP nanofibers increased within bicomponent fiber webs. Moreover, larger amounts of PVP nanofiber led to a lower electrostatic charge because of its hygroscopicity.[59,60] These results show that the fine control of wettability and electrostatic charge, which are important factors for drug delivery, wound dressing, and functional textiles, can be achieved by introducing different polymer species within fiber webs.[12,26−28] Since this combinatorial synergy of various polymer species can be further tailored using centrifugal multispinning, our system would open the potential of the multicomponent fiber webs for those applications.

To demonstrate the practicability of our process, we fabricated mask filters using PS nanofibers from our process considering the high demand of mask filters in recent years. First, we fabricated PS nanofiber-based filters for capturing fine dust with different amounts of PS nanofibers per unit area. The fabricated filter was easily integrated in the mask, as shown in Figure 4A. Capture efficiency and resistance of the filters were analyzed using an automated filter tester. Also, the filter performance was compared with that of filters from the literature and commercial products that are surgical mask, filters with grades of KF80 and KF94, and a mask fabricated by electrospun nanofibers (Mask-ES). Capture efficiency of the fabricated filters gradually increased from 82.97% to 96.63% as the weight of nanofiber increased (Figure 4B), showing a slightly higher performance than that of filters consisting of nanofibers with a similar average diameter (∼500 nm; Table S2).[61−66] Moreover, the performance is almost equal to that of commercial filters with KF80 and KF94 grades, implying excellent performance of our filter made of fibers spun by a centrifugal multispinning system. For the particle removal, inertial impaction and interception effect may be dominant among the well-established mechanisms (Figure 4C) considering that the average aerosol size corresponds to submicroscale. However, we cannot completely exclude the contribution of other filtration mechanisms that account for the removal of particulate matters of $O(100)$ nm to $O(10)$ μm because the test aerosol is not perfectly monodisperse. Meanwhile, resistance of the filters was relatively high compared to that of most filters in the literature, which may be due to the high flow velocity of the test condition. Actually, at the same face velocity, our filters demonstrated similar pressure drops with those of commercially available products, which shows a potential for the commercial use of PS nanofiber-based filters.

https://dx.doi.org/10.1021/acsmacrolett.0c00829
ACS Macro Lett. 2021, 10, 382−388

Compared to our filters and other products, Mask-ES showed extremely high resistance, and it may be due to the highly compact nanofiber network. Since the PS nanofiber-based filters have a small fraction of merged fibers with microscale, those large structures may lead to reduced resistance by introducing the cavity within the filter media.[67,68] We also examined the water droplet-blocking ability of the fabricated filters together with commercial products to demonstrate a potential of nanofiber-based filter to block viruses which spread by droplets (Figures 4D and S14). The test was performed under KF-antidroplet test conditions. As a result, no water droplet reached the bottom after 30 min, showing the outstanding droplet-blocking ability of our filters, like most of the other commercial products, except a surgical mask. It is due to the fact that the PS nanofiber web has a fine network and a nearly superhydrophobic nature, displaying a large contact angle of 145°. The results clearly demonstrate that the PS nanofiber-based filter can be employed for a mask filter to capture fine dust and infectious viruses, which spread by droplets, such as coronavirus.

For the mass production of a polymer nanofiber and an extension of nanofiber applications, a centrifugal multispinning system has been developed for the first time. Using a single subdisk of the novel spinneret, various polymer species, including PS, PMMA, and PVP, were successfully spun to micro- and nanofibers with a gram-scale production. Mass producibility and scalability of the system for the preparation of nanofibers were demonstrated using multiple subdisks by comparing the electrospinning process. Multicomponent fiber webs using PS and PVP solutions were also prepared, and the contact angle and electrostatic charge of the webs were finely controlled by varying the relative amount of PS to PVP. To demonstrate the applicability of produced fibers, the PS nanofibers were employed for mask filter application, and the fabricated filters showed high capture efficiency and outstanding blocking ability against water droplets, which show the potential of a nanofiber-based mask filter to capture fine dust and infectious viruses.

■ ASSOCIATED CONTENT

Supporting Information

The Supporting Information is available free of charge at https://pubs.acs.org/doi/10.1021/acsmacrolett.0c00829.

Experimental section: materials, centrifugal spinning of polymer nanofiber, electrospinning of polymer nanofiber, fabrication of mask filter and water blocking test, and characterization. Data section: size distribution of PS fibers, SEM images of PMMA and PVP fibers, SEM images of PS nanofibers with different subdisks, results of electrospinning, SEM images of PVP nanofibers with different flow rates, cospinning results at the same subdisk, and electrostatic charge of multicomponent fiber webs (PDF)

■ AUTHOR INFORMATION

Corresponding Author

Do Hyun Kim − *Department of Chemical and Biomolecular Engineering, Korea Advanced Institute of Science and Technology (KAIST), Yuseong-gu, Daejeon 34141, Republic of Korea;* orcid.org/0000-0001-8631-2790; Email: dohyun.kim@kaist.edu

Authors

Byeong Eun Kwak − *Department of Chemical and Biomolecular Engineering, Korea Advanced Institute of Science and Technology (KAIST), Yuseong-gu, Daejeon 34141, Republic of Korea;* orcid.org/0000-0002-3781-277X

Hyo Jeong Yoo − *Department of Chemical and Biomolecular Engineering, Korea Advanced Institute of Science and Technology (KAIST), Yuseong-gu, Daejeon 34141, Republic of Korea;* orcid.org/0000-0001-7088-8760

Eungjun Lee − *Department of Chemical and Biomolecular Engineering, Korea Advanced Institute of Science and Technology (KAIST), Yuseong-gu, Daejeon 34141, Republic of Korea*

Complete contact information is available at: https://pubs.acs.org/10.1021/acsmacrolett.0c00829

Notes

The authors declare no competing financial interest.

■ ACKNOWLEDGMENTS

This paper is based on research that has been conducted as part of the KAIST-funded Global Singularity Research Program for 2020.

■ REFERENCES

(1) Kim, K. H.; Kabir, E.; Kabir, S. A review on the human health impact of airborne particulate matter. *Environ. Int.* **2015**, *74*, 136−143.

(2) Guan, W. J.; Ni, Z. Y.; Hu, Y.; Liang, W. H.; Ou, C. Q.; He, J. X.; Liu, L.; Shan, H.; Lei, C. L.; Hui, D. S. C.; Du, B.; Li, L. J.; Zeng, G.; Yuen, K. Y.; Chen, R. C.; Tang, C. L.; Wang, T.; Chen, P. Y.; Xiang, J.; Li, S. Y.; Wang, J. L.; Liang, Z. J.; Peng, Y. X.; Wei, L.; Liu, Y.; Hu, Y. H.; Peng, P.; Wang, J. M.; Liu, J. Y.; Chen, Z.; Li, G.; Zheng, Z. J.; Qiu, S. Q.; Luo, J.; Ye, C. J.; Zhu, S. Y.; Zhong, N. S. China medical treatment expert group for COVID-19. Clinical characteristics of coronavirus disease 2019 in China. *N. Engl. J. Med.* **2020**, *382* (18), 1708−1720.

(3) Cheng, V. C.; Wong, S. C.; Chuang, V. W.; So, S. Y.; Chen, J. H.; Sridhar, S.; To, K. K.; Chan, J. F.; Hung, I. F.; Ho, P. L.; Yuen, K. Y. The role of community-wide wearing of face mask for control of coronavirus disease 2019 (COVID-19) epidemic due to SARS-CoV-2. *J. Infect.* **2020**, *81* (1), 107−114.

(4) Ullah, S.; Ullah, A.; Lee, J.; Jeong, Y.; Hashmi, M.; Zhu, C.; Joo, K. I.; Cha, H. J.; Kim, I. S. Reusability comparison of melt-blown vs nanofiber face mask filters for use in the coronavirus pandemic. *ACS Appl. Nano Mater.* **2020**, *3* (7), 7231−7241.

(5) Hashmi, M.; Ullah, S.; Kim, I. S. Copper oxide (CuO) loaded polyacrylonitrile (PAN) nanofiber membranes for antimicrobial breath mask applications. *Curr. Res. Biotechnol.* **2019**, *1*, 1−10.

(6) Li, X.; Gong, Y. Design of polymeric nanofiber gauze mask to prevent inhaling PM2.5 particles from haze pollution. *J. Chem.* **2015**, *2015*, 1−5.

(7) Xue, J.; Wu, T.; Dai, Y.; Xia, Y. Electrospinning and electrospun nanofibers: methods, materials, and applications. *Chem. Rev.* **2019**, *119* (8), 5298−5415.

(8) Subbiah, T.; Bhat, G. S.; Tock, R. W.; Parameswaran, S.; Ramkumar, S. S. Electrospinning of nanofibers. *J. Appl. Polym. Sci.* **2005**, *96* (2), 557−569.

(9) Khalid, B.; Bai, X.; Wei, H.; Huang, Y.; Wu, H.; Cui, Y. Direct blow-spinning of nanofibers on a window screen for highly efficient PM2.5 removal. *Nano Lett.* **2017**, *17* (2), 1140−1148.

(10) Rogalski, J. J.; Bastiaansen, C. W. M.; Peijs, T. Rotary jet spinning review - a potential high yield future for polymer nanofibers. *Nanocomposites* **2017**, *3* (4), 97−121.

(11) Zhang, X.; Lu, Y. Centrifugal spinning: an alternative approach to fabricate nanofibers at high speed and low cost. *Polym. Rev.* **2014**, *54* (4), 677−701.
(12) Wang, L.; Ahmad, Z.; Huang, J.; Li, J.-S.; Chang, M.-W. Multi-compartment centrifugal electrospinning based composite fibers. *Chem. Eng. J.* **2017**, *330*, 541−549.
(13) Gonzalez, G. M.; MacQueen, L. A.; Lind, J. U.; Fitzgibbons, S. A.; Chantre, C. O.; Huggler, I.; Golecki, H. M.; Goss, J. A.; Parker, K. K. Production of synthetic, para-aramid and biopolymer nanofibers by immersion rotary jet-spinning. *Macromol. Mater. Eng.* **2017**, *302*, 1600365.
(14) Loordhuswamy, A. M.; Krishnaswamy, V. R.; Korrapati, P. S.; Thinakaran, S.; Rengaswami, G. D. Fabrication of highly aligned fibrous scaffolds for tissue regeneration by centrifugal spinning technology. *Mater. Sci. Eng., C* **2014**, *42*, 799−807.
(15) Wang, L.; Chang, M.-W.; Ahmad, Z.; Zheng, H.; Li, J.-S. Mass and controlled fabrication of aligned PVP fibers for matrix type antibiotic drug delivery systems. *Chem. Eng. J.* **2017**, *307*, 661−669.
(16) Liu, Y. J.; Tan, J.; Yu, S. Y.; Yousefzadeh, M.; Lyu, T. T.; Jiao, Z. W.; Li, H. Y.; Ramakrishna, S. High-efficiency preparation of polypropylene nanofiber by melt differential centrifugal electrospinning. *J. Appl. Polym. Sci.* **2020**, *137*, 48299.
(17) Buzgo, M.; Rampichova, M.; Vocetkova, K.; Sovkova, V.; Lukasova, V.; Doupnik, M.; Mickova, A.; Rustichelli, F.; Amler, E. Emulsion centrifugal spinning for production of 3D drug releasing nanofibres with core/shell structure. *RSC Adv.* **2017**, *7* (3), 1215−1228.
(18) Yang, Y.; Zheng, N.; Zhou, Y.; Shan, W.; Shen, J. Mechanistic study on rapid fabrication of fibrous films via centrifugal melt spinning. *Int. J. Pharm.* **2019**, *560*, 155−165.
(19) Kancheva, M.; Toncheva, A.; Manolova, N.; Rashkov, I. Advanced centrifugal electrospinning setup. *Mater. Lett.* **2014**, *136*, 150−152.
(20) Chen, H.; Li, X.; Li, N.; Yang, B. Electrostatic-assisted centrifugal spinning for continuous collection of submicron fibers. *Text. Res. J.* **2017**, *87* (19), 2349−2357.
(21) Müller, F.; Jokisch, S.; Bargel, H.; Scheibel, T. Centrifugal electrospinning enables the production of meshes of ultrathin polymer fibers. *ACS Appl. Polym. Mater.* **2020**, *2*, 4360−4367.
(22) Lu, Y.; Fu, K.; Zhang, S.; Li, Y.; Chen, C.; Zhu, J.; Yanilmaz, M.; Dirican, M.; Zhang, X. Centrifugal spinning: a novel approach to fabricate porous carbon fibers as binder-free electrodes for electric double-layer capacitors. *J. Power Sources* **2015**, *273*, 502−510.
(23) Doan, H. N.; Nguyen, D. K.; Vo, P. P.; Hayashi, K.; Kinashi, K.; Sakai, W.; Tsutsumi, N.; Huynh, D. P. Facile and scalable fabrication of porous polystyrene fibers for oil removal by centrifugal spinning. *ACS Omega* **2019**, *4* (14), 15992−16000.
(24) Leng, G.; Zhang, X.; Shi, T.; Chen, G.; Wu, X.; Liu, Y.; Fang, M.; Min, X.; Huang, Z. Preparation and properties of polystyrene/silica fibres flexible thermal insulation materials by centrifugal spinning. *Polymer* **2019**, *185*, 121964.
(25) Zhou, H.; Tang, Y.; Wang, Z.; Zhang, P.; Zhu, Q. Cotton-like micro- and nanoscale poly(lactic acid) nonwoven fibers fabricated by centrifugal melt-spinning for tissue engineering. *RSC Adv.* **2018**, *8* (10), 5166−5179.
(26) Yoo, H. S.; Kim, T. G.; Park, T. G. Surface-functionalized electrospun nanofibers for tissue engineering and drug delivery. *Adv. Drug Delivery Rev.* **2009**, *61* (12), 1033−1042.
(27) Chen, M. L.; Besenbacher, F. Light-driven wettability changes on a photoresponsive electrospun mat. *ACS Nano* **2011**, *5*, 1549−1555.
(28) Lee, M. W.; An, S.; Joshi, B.; Latthe, S. S.; Yoon, S. S. Highly efficient wettability control via three-dimensional (3D) suspension of titania nanoparticles in polystyrene nanofibers. *ACS Appl. Mater. Interfaces* **2013**, *5* (4), 1232−1239.
(29) Wei, L.; Sun, R.; Liu, C.; Xiong, J.; Qin, X. Mass production of nanofibers from needleless electrospinning by a novel annular spinneret. *Mater. Des.* **2019**, *179*, 107885.
(30) Dosunmu, O. O.; Chase, G. G.; Kataphinan, W.; Reneker, D. H. Electrospinning of polymer nanofibres from multiple jets on a porous tubular surface. *Nanotechnology* **2006**, *17*, 1123−1127.
(31) Zhou, F. L.; Gong, R. H.; Porat, I. Polymeric nanofibers via flat spinneret electrospinning. *Polym. Eng. Sci.* **2009**, *49*, 2475−2481.
(32) Varabhas, J. S.; Chase, G. G.; Reneker, D. H. Electrospun nanofibers from a porous hollow tube. *Polymer* **2008**, *49*, 4226−4229.
(33) Tomaszewski, W.; Szadkowski, M. Investigation of electrospinning with the use of a multi-jet electrospinning head. *Fibres Text. East. Eur.* **2005**, *13*, 22−26.
(34) Niu, H.; Wang, X.; Lin, T. Needleless electrospinning: influences of fibre generator geometry. *J. Text. Inst.* **2012**, *103*, 787−794.
(35) Niu, H.; Lin, T.; Wang, X. Needleless electrospinning. I. a comparison of cylinder and disk nozzles. *J. Appl. Polym. Sci.* **2009**, *114*, 3524−3530.
(36) Liu, S.-L.; Huang, Y.-Y.; Zhang, H.-D.; Sun, B.; Zhang, J.-C.; Long, Y.-Z. Needleless electrospinning for large scale production of ultrathin polymer fibres. *Mater. Res. Innovations* **2014**, *18* (sup4), S4-833−S4-837.
(37) Moon, S.; Gil, M.; Lee, K. J. Syringeless electrospinning toward versatile fabrication of nanofiber Web. *Sci. Rep.* **2017**, *7*, 41424.
(38) Wang, X.; Lin, T.; Wang, X. Scaling up the production rate of nanofibers by needleless electrospinning from multiple ring. *Fibers Polym.* **2014**, *15*, 961−965.
(39) Wei, L.; Liu, C.; Mao, X.; Dong, J.; Fan, W.; Zhi, C.; Qin, X.; Sun, R. Multiple-jet needleless electrospinning approach via a linear flume spinneret. *Polymers* **2019**, *11*, 2052.
(40) Niu, H.; Wang, X.; Lin, T. Upward needleless electrospinning of nanofibers. *J. Eng. Fibers Fabr.* **2012**, *7*, 17−22.
(41) Holopainen, J.; Penttinen, T.; Santala, E.; Ritala, M. Needleless electrospinning with twisted wire spinneret. *Nanotechnology* **2015**, *26*, 025301.
(42) He, H. J.; Liu, C. K.; Molnar, K. A novel needleless electrospinning system using a moving conventional yarn as the spinneret. *Fibers Polym.* **2018**, *19*, 1472−1478.
(43) Zheng, G.; Jiang, J.; Chen, D.; Liu, J.; Liu, Y.; Zheng, J.; Wang, X.; Li, W. Multinozzle high efficiency electrospinning with the constraint of sheath gas. *J. Appl. Polym. Sci.* **2019**, *136*, 47574.
(44) Zhang, Y.; Cheng, Z.; Han, Z.; Zhao, S.; Zhao, X.; Kang, L. Stable Multi-Jet Electrospinning with high throughput using the bead structure nozzle. *RSC Adv.* **2018**, *8*, 6069−6074.
(45) Fang, S. P.; Jao, P. F.; Senior, D. E.; Kim, K. T.; Yoon, Y. K. Study on high throughput nanomanufacturing of photopatternable nanofibers using tube nozzle electrospinning with multi-tubes and multi-nozzles. *Micro Nano Syst. Lett.* **2017**, *5*, na.
(46) Pu, C.; He, J.; Cui, S.; Gao, W. Double-nozzle air-jet electrospinning for nanofiber fabrication. *J. Appl. Polym. Sci.* **2014**, *131*, 40040.
(47) Liu, Z.; Ang, K. K. J.; He, J. Needle-disk electrospinning inspired by natural point discharge. *J. Mater. Sci.* **2017**, *52*, 1823−1830.
(48) Tang, S.; Zeng, Y.; Wang, X. Splashing needleless electrospinning of nanofibers. *Polym. Eng. Sci.* **2010**, *50*, 2252−2257.
(49) Kumar, A.; Wei, M.; Barry, C.; Chen, J.; Mead, J. Controlling fiber repulsion in multijet electrospinning for higher throughput. *Macromol. Mater. Eng.* **2010**, *295*, 701−708.
(50) Wang, X.; Xu, W. Effect of experimental parameters on needleless electrospinning from a conical wire coil. *J. Appl. Polym. Sci.* **2012**, *123*, 3703−3709.
(51) Badrossamay, M. R.; McIlwee, H. A.; Goss, J. A.; Parker, K. K. Nanofiber assembly by rotary jet-spinning. *Nano Lett.* **2010**, *10* (6), 2257−2261.
(52) Mellado, P.; McIlwee, H. A.; Badrossamay, M. R.; Goss, J. A.; Mahadevan, L.; Parker, K. K. A simple model for nanofiber formation by rotary jet-spinning. *Appl. Phys. Lett.* **2011**, *99* (20), 203107.
(53) Li, Y.; Zhao, H.; Yang, M. TiO2 nanoparticles supported on PMMA nanofibers for photocatalytic degradation of methyl orange. *J. Colloid Interface Sci.* **2017**, *508*, 500−507.

https://dx.doi.org/10.1021/acsmacrolett.0c00829
ACS Macro Lett. 2021, 10, 382−388

(54) Zupancic, S.; Sinha-Ray, S.; Sinha-Ray, S.; Kristl, J.; Yarin, A. L. Long-term sustained ciprofloxacin release from PMMA and hydrophilic polymer blended banofibers. *Mol. Pharmaceutics* **2016**, *13* (1), 295−305.
(55) Mercante, L. A.; Facure, M. H. M.; Locilento, D. A.; Sanfelice, R. C.; Migliorini, F. L.; Mattoso, L. H. C.; Correa, D. S. Solution blow spun PMMA nanofibers wrapped with reduced graphene oxide as an efficient dye adsorbent. *New J. Chem.* **2017**, *41* (17), 9087−9094.
(56) Jin, Y.; Hwang, S.; Ha, H.; Park, H.; Kang, S.-W.; Hyun, S.; Jeon, S.; Jeong, S.-H. Buckled Au@PVP nanofiber networks for highly transparent and stretchable conductors. *Adv. Electron. Mater.* **2016**, *2*, 1500302.
(57) Jiang, Y. N.; Mo, H. Y.; Yu, D. G. Electrospun drug-loaded core-sheath PVP/zein nanofibers for biphasic drug release. *Int. J. Pharm.* **2012**, *438*, 232−239.
(58) Liu, Y.; Huang, H.; Wang, L.; Cai, D.; Liu, B.; Wang, D.; Li, Q.; Wang, T. Electrospun CeO2 nanoparticles/PVP nanofibers based high-frequency surface acoustic wave humidity sensor. *Sens. Actuators, B* **2016**, *223*, 730−737.
(59) Montgomery, J. F.; Green, S. I.; Rogak, S. N. Impact of relative humidity on HVAC filters loaded with hygroscopic and non-hygroscopic particles. *Aerosol Sci. Technol.* **2015**, *49* (5), 322−331.
(60) De Vrieze, S.; Van Camp, T.; Nelvig, A.; Hagström, B.; Westbroek, P.; De Clerck, K. The effect of temperature and humidity on electrospinning. *J. Mater. Sci.* **2009**, *44* (5), 1357−1362.
(61) Feng, J. P.; Wang, J.; Hwang, W. T.; Jo, Y. M. Characterization of filter media prepared from aligned nanofibers for fine dust screen. *J. Appl. Polym. Sci.* **2019**, *136*, 48166.
(62) Liu, H.; Zhang, S.; Liu, L.; Yu, J.; Ding, B. A fluffy dual-network structured nanofiber/net filter enables high-efficiency air filtration. *Adv. Funct. Mater.* **2019**, *29*, 1904108.
(63) Wang, N.; Zhu, Z.; Sheng, J.; Al-Deyab, S. S.; Yu, J.; Ding, B. Superamphiphobic nanofibrous membranes for effective filtration of fine particles. *J. Colloid Interface Sci.* **2014**, *428*, 41−48.
(64) Wang, N.; Raza, A.; Si, Y.; Yu, J.; Sun, G.; Ding, B. Tortuously structured polyvinyl chloride/polyurethane fibrous membranes for high-efficiency fine particulate filtration. *J. Colloid Interface Sci.* **2013**, *398*, 240−246.
(65) Al-Attabi, R.; Dumee, L. F.; Kong, L.; Schütz, J. A.; Morsi, Y. High efficiency poly(acrylonitrile) electrospun nanofiber membranes for airborne nanomaterials filtration. *Adv. Eng. Mater.* **2018**, *20*, 1700572.
(66) Tan, N. P. B.; Paclijan, S. S.; Ali, H. N. M.; Hallazgo, C. M. J. S.; Lopez, C. J. F.; Ebora, Y. C. Solution blow spinning (SBS) nanofibers for composite air filter masks. *ACS Appl. Nano Mater.* **2019**, *2*, 2475−2483.
(67) Yang, Y.; Zhang, S.; Zhao, X.; Yu, J.; Ding, B. Sandwich structured polyamide-6/polyacrylonitrile nanonets/bead-on-string composite membrane for effective air filtration. *Sep. Purif. Technol.* **2015**, *152*, 14−22.
(68) Choi, H. J.; Kumita, M.; Hayashi, S.; Yuasa, H.; Kamiyama, M.; Seto, T.; Tsai, C. J.; Otani, Y. Filtration properties of nanofiber/microfiber mixed filter and prediction of its performance. *Aerosol Air Qual. Res.* **2017**, *17*, 1052−1062.

https://dx.doi.org/10.1021/acsmacrolett.0c00829
ACS Macro Lett. 2021, 10, 382−388